



Cite this: *J. Anal. At. Spectrom.*, 2017, **32**, 562

GEOTRACES inter-calibration of the stable silicon isotope composition of dissolved silicic acid in seawater

Patricia Grasse,^{*ab} Mark A. Brzezinski,^{*b} Damien Cardinal,^c Gregory F. de Souza,^d Per Andersson,^e Ivya Closset,^c Zhimian Cao,^f Minhan Dai,^f Claudia Ehlert,^g Nicolas Estrade,^{†h} Roger François,^h Martin Frank,^a Guibin Jiang,ⁱ Janice L. Jones,^b Ellen Kooijman,^e Qian Liu,ⁱ Dawei Lu,ⁱ Katharina Pahnke,^g Emanuel Ponzevera,^j Melanie Schmitt,^e Xiaole Sun,^{‡k} Jill N. Sutton,^l François Thil,^m Dominique Weis,^h Florian Wetzel,^d Anyu Zhang,ⁿ Jing Zhangⁿ and Zhouling Zhang^f

The first inter-calibration study of the stable silicon isotope composition of dissolved silicic acid in seawater, $\delta^{30}\text{Si}(\text{OH})_4$, is presented as a contribution to the international GEOTRACES program. Eleven laboratories from seven countries analyzed two seawater samples from the North Pacific subtropical gyre (Station ALOHA) collected at 300 m and at 1000 m water depth. Sampling depths were chosen to obtain samples with a relatively low ($9 \mu\text{mol L}^{-1}$, 300 m) and a relatively high ($113 \mu\text{mol L}^{-1}$, 1000 m) silicic acid concentration as sample preparation differs for low- and high-concentration samples. Data for the 1000 m water sample were not normally distributed so the median is used to represent the central tendency for the two samples. Median $\delta^{30}\text{Si}(\text{OH})_4$ values of $+1.66\text{‰}$ for the low-concentration sample and $+1.25\text{‰}$ for the high-concentration sample were obtained. Agreement among laboratories is overall considered very good; however, small but statistically significant differences among the mean isotope values obtained by different laboratories were detected, likely reflecting inter-laboratory differences in chemical preparation including pre-concentration and purification methods together with different volumes of seawater analyzed, and the use of different mass spectrometers including the Neptune MC-ICP-MS (Thermo FisherTM, Germany), the Nu Plasma MC-ICP-MS (Nu InstrumentsTM, Wrexham, UK), and the FinniganTM (now Thermo FisherTM, Germany) MAT 252 IRMS. Future studies analyzing $\delta^{30}\text{Si}(\text{OH})_4$ in seawater should also analyze and report values for these same two reference waters in order to facilitate comparison of data generated among and within laboratories over time.

Received 16th August 2016
Accepted 1st December 2016

DOI: 10.1039/c6ja00302h

www.rsc.org/jaas

^aGEOMAR, Helmholtz Centre for Ocean Research Kiel, Ocean Circulation and Climate Dynamics, Wischhofstr. 1-3, 24148 Kiel, Germany

^bMarine Science Institute, Department of Ecology, Evolution, and Marine Biology, University of California, Santa Barbara, CA 93106, USA. E-mail: mark.brzezinski@lifesci.ucsb.edu

^cSorbonne Universités (UPMC, Univ Paris 06)-CNRS-IRD-MNHN, LOCEAN Laboratory, 4 place Jussieu, F-75005 Paris, France

^dETH Zurich, Institute of Geochemistry and Petrology, Clausiusstrasse 25, 8092 Zürich, Switzerland

^eSwedish Museum of Natural History, Department of Geosciences, 104 05 Stockholm, Sweden

^fState Key Laboratory of Marine Environmental Science, Xiamen University, Xiamen, China

^gMax Planck Research Group for Marine Isotope Geochemistry, Institute for Chemistry and Biology of the Marine Environment (ICBM), University of Oldenburg, Carl-von-Ossietzky-Str. 9-11, 26129 Oldenburg, Germany

^hUniversity of British Columbia, Pacific Center for Isotopic and Geochemical Research, Department of Earth, Ocean and Atmospheric Sciences, Vancouver, British Columbia, Canada V6T 1Z4

ⁱState Key Laboratory of Environmental Chemistry & Ecotoxicology, Research Center for Eco-Environmental Sciences, Chinese Academy of Sciences, 18 Shuangqing Road, Haidian District, Beijing 100085, China

^jUnité de Recherche Géosciences Marines, IFREMER, 29870, Plouzané, France

^kDepartment of Environmental Science and Analytical Chemistry, Stockholm University, Stockholm, Sweden

^lUniversité de Brest, CNRS, IRD, IFREMER, LEMAR, IUEM, Rue Dumont d'Urville, 29870, Plouzané, France

^mLSCE/IPSL – Laboratoire des Sciences du Climat et de l'Environnement, Laboratoire CEA-CNRS-UVSQ, Bât 12, Domaine du CNRS, Avenue de la Terrasse, F-91198 Gif sur Yvette Cedex, France

ⁿState Key Laboratory of Estuarine and Coastal Research, East China Normal University, Shanghai 200062, China

[†] Present address: LEGOS, Equipe TIM, Observatoire Midi Pyrénées, 14 av Edouard Belin, 31400 Toulouse, France.

[‡] Current affiliation: Baltic Sea Center, Stockholm University, 106 91 Stockholm, Sweden.

1 Introduction

The stable isotope composition of silicon in dissolved silicic acid in seawater, $\delta^{30}\text{Si}(\text{OH})_4$, is a powerful tool for understanding the silicon cycle in the ocean as it reflects changes in the biological utilization of silicic acid, $\text{Si}(\text{OH})_4$, by diatoms in surface water as well as water mass mixing. $\delta^{30}\text{Si}$ measurements in both $\text{Si}(\text{OH})_4$ and in biogenic silica are essential to fully understand the marine Si cycle, in particular to characterize Si sources and sinks in order to better constrain the Si budget in the ocean.¹ Besides their importance in understanding the present day Si cycle, $\delta^{30}\text{Si}$ measurements are increasingly being used to assess past changes through the isotopic analysis of Si in biogenic silica within diatom frustules and within sponge spicules from marine sediments.^{2–4}

Beginning with the first report of $\delta^{30}\text{Si}$ measurements in natural waters by De La Rocha *et al.*,⁵ there has been a growing number of publications, especially in the past five years, reporting $\delta^{30}\text{Si}(\text{OH})_4$ values from marine systems, covering locations in the Southern, Atlantic, Pacific, and Indian Oceans as well as large estuaries.^{6–12} This data set is anticipated to grow as part of the international GEOTRACES program that seeks to understand the global-scale distributions of trace elements and their isotopes in the marine environment (<http://www.geotraces.org>). All Si isotope data obtained by the GEOTRACES and other programs need to be fully comparable in order to better understand Si isotope systematics across the global ocean, and to validate models of the global marine $\delta^{30}\text{Si}(\text{OH})_4$ distribution.^{13–16} However, such efforts are challenged by the lack of seawater reference material of known $\delta^{30}\text{Si}(\text{OH})_4$ to intercalibrate data generated by different laboratories or within a single laboratory through time, as is currently only possible for solid siliceous materials.¹⁷

The procedures and instrumentation used in stable Si isotope analysis have evolved substantially over the last two decades. The first precise $\delta^{30}\text{Si}$ measurements of marine dissolved and particulate Si were conducted using a VG Prism gas source isotope ratio mass spectrometer (IRMS) with samples prepared using a manual fluorination line that employed F_2 gas to convert Si recovered from either seawater or from biogenic silica as solid SiO_2 to SiF_4 gas.¹⁸ IRMS methods have since been improved with SiF_4 now produced from acid decomposition of Cs_2SiF_6 in an automated process employing a modified Kiel III carbonate device and a MAT 252 IRMS.¹⁹ The first multi-collector inductively coupled plasma mass spectrometer MC-ICP-MS (Nu Plasma™, Nu Instruments, Wrexham, UK) measurements were performed by De La Rocha.²⁰ This method was improved by Cardinal *et al.*,²¹ who used a dry-plasma mode and Mg doping to correct for mass bias. These early MC-ICP-MS studies measured $\delta^{29}\text{Si}$ (calculated from $^{29}\text{Si}/^{28}\text{Si}$; cf. eqn (1)) to avoid the polyatomic interference of $^{14}\text{N}^{16}\text{O}^+$ on m/z ^{30}Si , but this interference has since been overcome by the higher resolving power of new instruments, with all current studies reporting $\delta^{30}\text{Si}$ values. However, it is possible to convert between the two values using the relationship $\delta^{29}\text{Si} = 0.51 \times \delta^{30}\text{Si}$, assuming pure kinetic isotope fractionation of Si.¹⁷ $\delta^{30}\text{Si}$

isotope measurements have now been successfully performed on a Neptune and Neptune Plus MC-ICP-MS (Thermo Fisher™, Germany^{22,23}), various types of MC-ICP-MS produced by Nu Instruments™ (Wrexham, UK), including a Nu Plasma,⁶ Nu Plasma HR,²⁴ (2013), and the Nu Plasma 1700 high-resolution MC-ICP-MS,⁷ as well as on a Finnigan™ MAT 252 IRMS.²⁵

Both mass spectrometry types (MC-ICP-MS and IRMS) produce reliable $\delta^{30}\text{Si}(\text{OH})_4$ data with a long-term reproducibility of 0.1–0.2‰ (2 s.d.).^{10,21} A major advantage of MC-ICP-MS over current IRMS methods is the significantly lower sample mass (~0.2 μmol Si) required for analysis compared to current methods using IRMS that require approximately 10 times higher mass, necessitating a much larger sampling volume which may become prohibitively large for Si-depleted near-surface waters. On the other hand, IRMS measurements have fewer problems with molecular mass interferences, given that Si is measured in the form of SiF_3^+ at m/z 85, 86, 87. Interference from SiOF_2 with $^{29}\text{Si}^{18}\text{OF}_2^+$, $^{30}\text{Si}^{17}\text{OF}_2^+$ at m/z 85 and $^{30}\text{Si}^{18}\text{OF}_2^+$ at m/z 86 is possible and can be detected by the presence of the same oxyfluorides containing the far more abundant ^{16}O and ^{28}Si atoms at m/z 82, 83 and 84. Such interferences are rare with current sample preparation methods. With MC-ICP-MS, Si is measured as elemental Si with potential polyatomic interferences from C, H, O and N (*e.g.* $^{14}\text{N}_2$, $^{14}\text{N}_2\text{H}$, $^{12}\text{C}^{16}\text{O}$, $^{12}\text{C}^{16}\text{H}^{16}\text{O}$, $^{14}\text{N}^{16}\text{O}$) that can bias beam intensities for m/z ^{28}Si , ^{29}Si and ^{30}Si . Care must also be taken to eliminate matrix effects that may be caused by remnants of dissolved organic matter and anions such as sulfate.^{26,27} For a detailed comparison between IRMS and MC-ICP-MS measurements see Reynolds *et al.*¹⁷

Recent studies of $\delta^{30}\text{Si}(\text{OH})_4$ distribution in deep waters (>1000 m) in the Atlantic Ocean by de Souza *et al.*²⁷ and by Brzezinski and Jones¹⁰ highlight the need for improved intercalibration among laboratories measuring $\delta^{30}\text{Si}(\text{OH})_4$. $\delta^{30}\text{Si}(\text{OH})_4$ values at these depths are expected to be invariant over the relatively short period of time separating these studies, yet comparison of $\delta^{30}\text{Si}(\text{OH})_4$ data between these two studies showed a near constant offset of approximately 0.22‰ between samples of comparable silicic acid concentration (see Fig. 2 in Brzezinski and Jones¹⁰). Brzezinski and Jones¹⁰ could not explain the offset, as $\delta^{30}\text{Si}$ values for solid Si standards reported by both laboratories were in good agreement. Given that sample preparation methods for samples of solid and dissolved Si differ considerably^{7,28} and in view of the fact that seawater represents a complex matrix of anions and cations, the use of solid standards, and especially of relatively pure siliceous materials, cannot account for sample preparation biases arising during the preparation of seawater samples, motivating the establishment of reference seawaters for this purpose.

The only inter-laboratory calibration of Si isotope standards to date was conducted with solid Si material.¹⁷ In that study, 8 groups participated and obtained consensus mean $\delta^{30}\text{Si}$ values for high-purity Si solids ($\delta^{30}\text{Si}_{\text{Diatomite}}: +1.26 \pm 0.20\text{‰}$, $\delta^{30}\text{Si}_{\text{IRMM-018}}: -1.65 \pm 0.22\text{‰}$, $\delta^{30}\text{Si}_{\text{Big Batch}}: -10.48 \pm 0.54\text{‰}$, averages with 2 s.d. uncertainties). Those materials are now routinely analyzed and reported when presenting Si isotope data from natural waters, diatom frustules, sponge spicules and minerals. A few rock reference materials are also commonly used as $\delta^{30}\text{Si}$

isotopic standards to determine accuracy and reproducibility of solid samples with a complex matrix, especially BHVO-1 and BHVO-2.^{29,30} As exemplified by the offsets between studies measuring $\delta^{30}\text{Si}(\text{OH})_4$ in seawater discussed above, these standards are of limited use for identifying sample preparation biases among laboratories analyzing seawater Si isotopes.

In the following we present the first inter-laboratory calibration study for $\delta^{30}\text{Si}(\text{OH})_4$ using seawater samples with low ($\sim 9 \mu\text{mol L}^{-1}$) and high ($\sim 113 \mu\text{mol L}^{-1}$) $\text{Si}(\text{OH})_4$ concentration. The two main goals were to evaluate current reproducibility among laboratories and to establish $\delta^{30}\text{Si}(\text{OH})_4$ values for the samples so that they can be analyzed and reported as part of future studies to aid in comparing data generated among and within laboratories over time.

2 Methods

2.1 Seawater sampling

The seawater for the inter-calibration study was collected at Station ALOHA ($22^\circ 45' \text{N}$ latitude, $158^\circ 00' \text{W}$ longitude) in the North Pacific subtropical gyre. Two large volume seawater samples (60 L each) were collected during the Hawaii Ocean Time series (HOT) cruise 256 (October/November 2013) courtesy of the HOT program using the CTD/rosette sampler aboard the R/V Kilo Moana that was equipped with Niskin bottles and a Sea-Bird SBE-9/11 Plus CTD. Samples were collected from 300 m (ALOHA₃₀₀) and 1000 m (ALOHA₁₀₀₀) water depth in order to obtain samples with a low and with a high $\text{Si}(\text{OH})_4$ concentration based on the known increase in $[\text{Si}(\text{OH})_4]$ with depth at this location. For each sample seawater from replicate Niskin bottles was pooled in an acid-washed (10% HCl) polyethylene carboy and gravity-filtered into a second acid-washed carboy using AcroPak® filter capsules containing sequential 0.8/0.45 μm Supor® membrane filters that had been washed with trace-metal-grade HCl prior to use. Samples were not acidified or preserved as repeated measures of unpreserved samples show no change in either silicic acid concentration or silicon isotopic composition over a period of ten years when kept in the dark (Brzezinski, unpublished).

2.2 Sample preparation and silicon isotope measurements

At the University of California Santa Barbara (UCSB), the $\text{Si}(\text{OH})_4$ concentration of each sample was measured as described by Brzezinski and Nelson.³¹ Both ALOHA₃₀₀ and ALOHA₁₀₀₀ samples were then aliquoted into 50 mL acid-cleaned polypropylene screw cap tubes, and shipped in groups of 25 tubes each to participating laboratories.

In total, 11 laboratories from 7 countries participated in the study (Table 1). Each group used its own techniques and protocols for sample preparation and Si isotope measurements, as detailed in Table 4. In addition to analyzing the seawater samples, many groups also measured the solid secondary standards Big Batch and Diatomite used in the previous inter-calibration of siliceous solids by Reynolds *et al.*¹⁷

All groups used some form of scavenging or precipitation to concentrate Si from the ALOHA₃₀₀ sample and to remove major

seawater ions (*e.g.* Na^+ , Cl^- , SO_4^{2-}). All groups followed similar procedures for ALOHA₁₀₀₀ except for group 10 which did not pre-concentrate ALOHA₁₀₀₀. Several pre-concentration methods were used: (i) a Magnesium Induced Co-precipitation (MAGIC) method with sodium hydroxide;^{27,28,32} (ii) a Mg-induced co-precipitation with purified ammonia ($\text{NH}_3 \cdot \text{H}_2\text{O}$)³³ and (iii) a TEA-moly precipitation¹⁸ during which Si is precipitated as a triethylamine silico-molybdate complex. In the following we will refer to the chemical (NaOH, ammonia, TEA-moly) to describe the precipitation method. The most common precipitation method was NaOH, followed by ammonia and TEA-moly precipitation.

In order to further purify the samples, most groups using magnesium co-precipitation dissolved the magnesium hydroxide precipitate in a strong acid and then applied column chromatography, using either a cation exchange resin (AG50W-X8; Dowex 50W-X8, AG50W-X12, 200 to 400 mesh) or an anion exchange resin (AG1-X8). Samples precipitated as TEA-moly were purified by high-temperature combustion to solid SiO_2 in a platinum crucible, followed by the dissolution of the SiO_2 in HF and the precipitation of the dissolved Si as Cs_2SiF_6 .¹⁹ Depending on the chemical preparation and the mass spectrometer type, the sample volume needed for Si isotope measurements ranged from 8 mL to 2000 mL for ALOHA₃₀₀ and from 1 mL to 200 mL for ALOHA₁₀₀₀ with the largest seawater volume being required for measurements by IRMS. For an overview of the different chemical preparation methods, see Table 1. More details about chemical preparation and mass spectrometry methods are given in Table 4.

Si isotope measurements were performed on three different mass spectrometer types (Table 1). Four groups used a Neptune or Neptune Plus MC-ICP-MS (Thermo Fisher™, Germany), six groups a Nu Plasma MC-ICP-MS (Nu Instruments™, Wrexham, UK; including a Nu Plasma II MC-ICP-MS and a Nu Plasma 1700 HR-MC-ICP-MS) and one group employed a MAT 252 IRMS (Finnigan™, now Thermo Fisher™, Germany). The MC-ICP-MS measurements were performed on solutions containing 10–90 $\mu\text{mol L}^{-1}$ Si (0.35–2.5 ppm Si), which resulted in a 2–9 V ion beam (on a Faraday cup equipped with a $10^{11} \Omega$ resistor) for elemental Si with m/z of 28, the most abundant stable isotope of Si (atom% $^{28}\text{Si} = 92.229\%$).³⁴ Most MC-ICP-MS analyses were carried out in 'dry plasma mode' using one of three different desolvating nebulizer systems (CETAC Aridus II™, Nu Instruments DSN-100™, ESI Apex™) to remove the sample solvent before introduction into the plasma. Only 2 groups employed 'wet plasma mode' (Table 4), which avoids possible blank problems with the desolvating nebulizer system, but is less sensitive.²⁹ On the IRMS, samples are loaded into a modified Kiel III carbonate device as solid Cs_2SiF_6 (6 μmol Si) and decomposed to SiF_4 gas with 98% sulfuric acid. Electron ionization of SiF_4 in the instrument source creates SiF_3^+ ions measured at 85, 86 and 87 m/z (ref. 18 and 19) with a typical voltage of 4–8 V (on a Faraday cup with a $3 \times 10^8 \Omega$ resistor) at 85 m/z corresponding to $^{28}\text{Si}^{19}\text{F}_3^+$.

The intensity of the blank was generally below 1% of the sample signal across laboratories (Table 4). All measurements were performed using a standard-sample-bracketing method. For MC-ICP-MS measurements the standard employed was the

Table 1 Summary of the different participating laboratory groups and methods for sample preparation and mass spectrometry

No.	Lab	Country	Responsible person	Sample introduction	Mass spectrometry	Precipitation method	Further preparation	Extras	References
1	MPI Oldenburg	Germany	Claudia Ehlert, Katharina Pahnke	Wet-plasma	Neptune Plus	NaOH	Cation exchange resin (AG50W-X8)	H ₂ O ₂ /UV treatment/ Mg doping	Georg <i>et al.</i> 2006; Hughes <i>et al.</i> 2011
2	LOCEAN/LSCE	France	Damien Cardinal, Ivia Closset	Apex, dry-plasma	Neptune Plus	NaOH	Cation exchange resin (AG50W-X8)	Mg/SO ₄ ²⁻ – doping	Karl and Tien 1992; Georg <i>et al.</i> 2006; Hughes <i>et al.</i> 2011
3	Unité de Recherche Géosciences Marines, IFREMER and Université de Brest	France	Jill Sutton	Apex, dry-plasma	Neptune	TEA-moly	Anion exchange resin (AG1-X8)	Mg doping	Cardinal <i>et al.</i> 2005; Engström <i>et al.</i> 2006; de La Rocha <i>et al.</i> 2006; de LaRocha <i>et al.</i> 2011
4	ETH Zürich	Switzerland	Florian Wetzel, Gregory de Souza	DSN-100, dry-plasma	Nu Plasma 1700	NaOH	Cation exchange resin (AG50W-X8)		Georg <i>et al.</i> 2006; deSouza <i>et al.</i> 2012
5	Swedish Museum of Natural History	Sweden	Per Andersson, Xiaole Sun	Wet-plasma	Nu Plasma II	NaOH	Cation exchange resin (AG50W-X8)		Georg <i>et al.</i> 2006; Sun <i>et al.</i> 2014
6	GEOMAR Helmholtz Centre for Ocean Research Kiel	Germany	Patricia Grasse, Martin Frank	Aridus II, dry-plasma	Nu Plasma II	NaOH/NH ₄	Cation exchange resin (AG50W-X8)		Karl and Tien 1992; Georg <i>et al.</i> 2006; Zhang <i>et al.</i> 2014
7	University of British Columbia	Canada	Nicolas Estrade	Aridus II, dry-plasma	Nu Plasma 1700	NH ₄	Cation exchange resin (AG50W-X8)		Karl and Tien 1992; Zhang <i>et al.</i> 2014
8	University of California Santa Barbara	US	Janice Jones, Patricia Grasse, Mark Brzezinski	Dual-inlet gas-source	Kiel III MAT 252	TEA-moly	HF dissolution, then CsSiF ₆ precipitation		De LaRocha <i>et al.</i> 1996; Brzezinski <i>et al.</i> 2006
9	Xiamen University	China	Minhan Dai, Zouling Zang	Dry-plasma	Nu Plasma II	NaOH	Cation exchange resin (AG50W-X8)		Karl and Tien 1992; Georg <i>et al.</i> 2006
10	Research Center for Eco-Environmental Sciences, CAS Beijing	China	Qian Liu	DSN-100, dry-plasma	Nu Plasma II	NaOH	Cation exchange resin (Dowex 50W-X8)		Karl and Tien 1992; Georg <i>et al.</i> 2006
11	State Key Laboratory of Estuarine and Coastal Research, Shanghai	China	Anyu Zhang	Dry-plasma	Neptune	NH ₄	Cation exchange resin (Dowex 50W-X8)		Georg <i>et al.</i> 2006; Zhang <i>et al.</i> 2014; Zhang <i>et al.</i> 2015

Table 2 Summary of mean Si isotope values ($\delta^{30}\text{Si}$, $\delta^{29}\text{Si}$), the associated 2σ analytical uncertainty (2 s.d.), number of chemical preparations (N) and the number of measurements (n) obtained by each laboratory group for ALOHA₃₀₀ and ALOHA₁₀₀₀. Overall mean, uncertainty about the mean (2 s.d.), median as well as the interquartile deviation (IQD) for all groups are given at the bottom of the table. NaN indicates data not available (for a compilation of all measurements see Table 5)

Group no.	ALOHA ₃₀₀						ALOHA ₁₀₀₀							
	$\delta^{30}\text{Si}$	2 s.d.	$\delta^{29}\text{Si}$	2 s.d.	$\delta^{29}\text{Si}/\delta^{30}\text{Si}$	N	n	$\delta^{30}\text{Si}$	2 s.d.	$\delta^{29}\text{Si}$	2 s.d.	$\delta^{29}\text{Si}/\delta^{30}\text{Si}$	N	n
1	NaN	NaN	NaN	NaN	NaN	NaN	NaN	1.10	0.07	0.63	0.07	0.57	4	4
2	1.66	0.10	0.84	0.05	0.50	6	12	1.10	0.07	0.56	0.02	0.51	5	15
3	NaN	NaN	NaN	NaN	NaN	NaN	NaN	1.16	0.16	0.59	0.09	0.51	3	9
4	1.64	0.13	0.87	0.05	0.53	4	12	1.17	0.20	0.62	0.10	0.53	3	12
5	1.51	0.12	0.80	0.08	0.53	3	11	1.23	0.08	0.64	0.04	0.52	4	15
6	1.78	0.18	0.89	0.18	0.50	6	6	1.26	0.12	0.68	0.09	0.54	5	5
7	1.92	0.08	1.02	0.12	0.53	5	14	1.25	0.07	0.65	0.07	0.52	6	31
8	1.46	0.17	0.75	0.09	0.51	3	10	1.29	0.04	0.66	0.02	0.51	4	25
9	1.94	0.12	0.99	0.08	0.51	8	16	1.31	0.15	0.68	0.09	0.52	10	20
10	1.53	0.17	0.79	0.11	0.52	3	9	1.45	0.17	0.76	0.16	0.53	3	9
11	1.69	0.24	0.85	0.17	0.50	8	8	1.27	0.05	0.65	0.03	0.51	8	72
Mean	1.68		0.87		0.52			1.24		0.65		0.52		
2 s.d.	0.35		0.10					0.20		0.10				
Median	1.66		0.85					1.25		0.65				
Modal value	1.66		0.85					1.22		0.65				
IQD	0.13		0.05					0.05		0.02				

reference standard NBS28 or an in-house standard that had been calibrated against NBS28. For IRMS measurements samples were run against cryogenically purified commercial SiF₄ gas which had been calibrated against NBS28. NBS28 (NIST Reference Material 8546) is a silica sand that was obtained by the United States Geological Survey from the Corning Glass Company.

Si isotope compositions are reported in the δ -notation using the reference standard NBS28 in parts per thousand,

$$\delta^{30}\text{Si} = \left(\left(\frac{R_{\text{sample}}}{R_{\text{std}}} \right) - 1 \right) \times 1000 \quad (1)$$

where R_{sample} is the measured $^{30}\text{Si}/^{28}\text{Si}$ ratio of the sample and R_{std} is the measured $^{30}\text{Si}/^{28}\text{Si}$ ratio of the NBS28 standard.

Laboratories pre-concentrated each seawater sample 3 to 10 times. Each pre-concentration was considered to be a replicate when performing statistical tests and when evaluating the external reproducibility for each group (2 s.d., Tables 2 and 5). The analytical scheme applied to each pre-concentration was as follows: subsamples of each concentrate were analyzed between 1 and 12 times with the actual number of analyses performed listed as analytical replicates for each pre-concentration in Table 5. Analysis of the subsamples by both IRMS and MC-ICP-MS utilized a standard-sample-bracketing approach, which depending on the laboratory involved 15 to 60 measurements of the subsample bracketed by analyses of the standard. Each set of analytical replicates was averaged providing a mean value for each separate pre-concentration of ALOHA₃₀₀ and of ALOHA₁₀₀₀ performed by each laboratory (Table 5).

Analysis of variance (ANOVA) was used to test for difference among means with *post hoc* tests performed using Tukey's HSD (honest significant difference) method to control type I error rate across multiple comparisons. For each ANOVA Levene's method was used to test for the equality of variance among factors and the Shapiro-Wilk method was used to test that the residuals from

each ANOVA model were normally distributed. A significance level of $p = 0.05$ was used throughout. Residuals were normally distributed across all tests and will not be discussed further. However, in some cases the variance across factors was found not to be constant. In those cases, differences among means were re-evaluated using Welch's ANOVA that is not reliant on an

Table 3 Statistics for $\delta^{30}\text{Si}(\text{OH})_4$ values sorted by different instrument types and precipitation methods (for details see Table 4). NaN denotes sample not available

Grouped by instrument	ALOHA ₃₀₀			ALOHA ₁₀₀₀		
	Neptune	Nu	IRMS	Neptune	Nu	IRMS
Median	1.64	1.81	1.51	1.15	1.28	1.28
Mean	1.68	1.78	1.46	1.18	1.28	1.29
2 s.d.	0.19	0.36	0.17	0.18	0.18	0.04
Min	1.52	1.45	1.36	1.07	1.08	1.27
Max	1.86	2.05	1.52	1.30	1.55	1.31
N	14	29	3	20	31	4

Grouped by precipitation	ALOHA ₃₀₀			ALOHA ₁₀₀₀		
	NaOH	Ammonia	TEA-moly	NaOH	Ammonia	TEA-moly
Median	1.69	1.82	1.51	1.25	1.27	1.27
Mean	1.73	1.78	1.46	1.24	1.26	1.23
2 s.d.	0.34	0.30	0.17	1.25	0.06	0.16
Min	1.45	1.52	1.36	1.07	1.20	1.10
Max	2.05	1.97	1.52	1.55	1.30	1.31
N	30	13	3	32	16	7

Table 4 (a) Detailed overview of chemical preparation and measurement methods (Nu Plasma), (b) detailed overview of chemical preparation and measurement methods (Neptune), (c) detailed overview of chemical preparation and measurement methods (IRMS)

(a)	4	5	6	7	9	10
Group Sample vol. (ALOH _{A300})	50 mL	50 mL	30 mL	12 mL	15 mL	15 mL
Sample vol. (ALOH _{A1000})	10 mL	10 mL	10 mL	12 mL	10 mL	10 mL
Precipitation method	MAGIC Sodium hydroxide	MAGIC Ammonium hydroxide	MAGIC Ammonium & sodium hydroxide	MAGIC Ammonium hydroxide	MAGIC Sodium hydroxide	MAGIC Ammonium hydroxide
Column chemistry	Cation exchange resin AG50W-X8, 200–400 mesh	Cation exchange resin AG50W-X12	Cation exchange resin AG50W-X8, 200–400 mesh	Cation exchange resin AG50W-X8, 200–400 mesh	Cation exchange resin AG50W-X8, 200–400 mesh	Cation exchange resin Dowex 50W-X8
Amount Si (μg) introduced into machine	2.5 μg	0.6 to 1.6 μg	2.5 μg	1.4 μg	1.4 μg	1.8 μg
Mg doping (yes/no) Extras	No	No	No	No	No	Yes
Co-precipitation for ALOH _{A1000} and ALOH _{A300}	2.5 μg	0.6 to 1.6 μg	2.5 μg	1.4 μg	1.4 μg	1.8 μg
Mass spectrometer	Nu Plasma (1700) HR-MC-ICP-MS	Nu Plasma (II) MC-ICP-MS	Nu Plasma (II) MC-ICP-MS	Nu Plasma (1700) HR-MC-ICP-MS	Nu Plasma (II) MC-ICP-MS	Nu Plasma (II) MC-ICP-MS
Sample introduction	Desolvator DSN-100; PFA nebulizer; $\sim 75 \mu\text{L min}^{-1}$ uptake rate	Wet plasma, glass nebulizer, $\sim 100 \mu\text{L min}^{-1}$ uptake rate	Desolvator Cetac Aridus II, PFA nebulizer, $\sim 70 \mu\text{L min}^{-1}$ uptake rate	Desolvator Cetac Aridus II, PFA nebulizer, $\sim 100 \mu\text{L min}^{-1}$ uptake rate	Desolvation nebulizer system, PFA nebulizer, $\sim 80 \mu\text{L min}^{-1}$ uptake rate	Desolvation nebulizer (DSN-100), PFA nebulizer, $\sim 70 \mu\text{L min}^{-1}$ uptake rate
Cones Torch	Common Ni cones Semi-demountable quartz torch, alumina injector	Common Ni cones Glass	Common Ni cones Glass	Common Ni cones Glass	Common Ni cones Glass	Common Ni cones Glass
Measurement mode	High resolution	Medium resolution; $m/\Delta m$ 4000–7000	Medium resolution	High resolution	Medium resolution	Medium resolution
Standard-sample bracketing	Yes smp. repeated 5 times 1 block, 36 cycles of 5 s each	Yes smp. repeated 3 times 2 blocks, 20 cycles	Yes smp. repeated 4–5 times 1 block, 60 cycles	Yes smp. repeated 3 times 1 block, 25 cycles, 10 s	Yes smp. repeated 4–5 times 1 block, 20 cycles	Yes smp. repeated 3 times 4 blocks, 15 cycles
Measurement intensity (²⁸ Si) Blanks (²⁸ Si)	10 to 30 mV	2–3.5 V ppm^{-1}	4 V	9 V for 0.35 ppm Si	6 V	5.5 V ppm^{-1}
		10–30 mV	10 to 30 mV	40–100 mV, measured by OPZ	50 to 80 mV	16 to 36 mV

Table 4 (Contd.)

Instrument setting	Finnigan Mat 252 IRMS
Mass spec	Modified Kiel III inlet system, 98% sulfuric acid decomposition of Cs ₂ SiF ₆ to SiF ₄
Introduction	Standard-sample bracketing
Measurement mode	>3 replicates
	1 block, 20 cycles, 8 s integration time
	6 μmol
Amount Si introduced in the machine	2 V to 8 V
Measurement intensity (²⁸ SiF ₃ ⁺)	No blank
Blanks (²⁸ SiF ₃ ⁺)	

assumption of homogenous variances among factors with *post hoc* testing performed using False Discovery Rate procedures (q-FDR).^{35,36} q-FDR controls the expected proportion of type I errors rather than the probability that such errors will occur which can increase statistical power compared to family-wise error rate techniques for handling multiple comparisons.³⁵ Statistical analyses were performed using JMP 12 statistical software.

2.3 Mg doping and sulfate addition

Except for one laboratory, all measurements on Neptune mass spectrometers were performed with Mg doping of the sample, whereas only group 10 applied Mg doping to samples measured on a Nu Plasma instrument. Cardinal *et al.*²¹ showed that Mg isotope mass bias is constant relative to Si isotopes during a MC-ICP-MS analytical session and follows an exponential mass fractionation law. Si isotope ratios (³⁰Si/²⁸Si and ²⁹Si/²⁸Si) were corrected for mass bias by adding Mg(NO₃)₂ to samples and to standards just prior to measurement.^{21,29} Mg is added at a concentration that matches the Si content of standards and samples. Between each measurement of Si isotopes ²⁴Mg and ²⁵Mg and/or ²⁶Mg isotopes are measured in dynamic mode with the same integration time as for Si isotopes. The correction to the ³⁰Si/²⁸Si ratio (³⁰Si/²⁸Si)_{corr} is calculated as follows:

$$(^{30}\text{Si}/^{28}\text{Si})_{\text{corr}} = (^{30}\text{Si}/^{28}\text{Si})_{\text{meas}} \times (^{30}\text{Si}_{\text{AM}}/^{28}\text{Si}_{\text{AM}})^{\varepsilon_{\text{Mg}}} \quad (2)$$

where (³⁰Si/²⁸Si)_{meas} is the measured ratio, ³⁰Si_{AM} and ²⁸Si_{AM} are the atomic masses of ³⁰Si and ²⁸Si. ε_{Mg} is then calculated from the beam intensities on masses 26 and 24 as:

$$\varepsilon_{\text{Mg}} = \ln[(^{26}\text{Mg}_A/^{24}\text{Mg}_A)/(^{26}\text{Mg}/^{24}\text{Mg})_{\text{meas}}]/\ln[^{26}\text{Mg}_{\text{AM}}/^{24}\text{Mg}_{\text{AM}}] \quad (3)$$

where ²⁶Mg_A/²⁴Mg_A is the expected ratio of the natural abundances of the isotopes, (²⁶Mg/²⁴Mg)_{meas} is the measured ratio, and ²⁶Mg_{AM} and ²⁴Mg_{AM} are the atomic masses of ²⁶Mg and ²⁴Mg.

One laboratory (group 2) implemented sulfate doping to overcome the effects of the presence of seawater sulfate ions (Table 1). Van den Boorn *et al.*²⁶ were the first to report a significant isotopic bias due to the presence of SO₄²⁻ in rock samples after a cation chromatographic purification step. Such a bias was also observed by Hughes *et al.*³⁷ on freshwater samples of dissolved Si, although Georg *et al.*²⁸ and de Souza *et al.*²⁷ did not observe a significant matrix effect of SO₄²⁻ on their MC-ICP-MS analyses of Si isotopes from freshwater and seawater samples. In the present study several tests were made to optimize sulfate doping. For group 2, systematic and constant H₂SO₄ additions were performed as for Mg prior to the measurements on the ALOHA₁₀₀₀ sample and the NBS28 standard at 1 mmol L⁻¹, which should largely overcome the amount of seawater SO₄²⁻ remaining in the solutions. For the ALOHA₃₀₀ sample where group 2 processed 50 mL of seawater, systematic measurements of SO₄²⁻ were made *via ad hoc* doping to reach 1 mmol L⁻¹ H₂SO₄. Nitric acid and HCl were also added by group 2 to all samples and standards to reach final concentrations of 0.5 mol L⁻¹ each in order to overcome the influence of residual seawater nitrate and chloride ions.

Table 5 (a) Measurements of $\delta^{30}\text{Si}(\text{OH})_4$ and $\delta^{29}\text{Si}(\text{OH})_4$ by each laboratory group for ALOHA₁₀₀₀. The means of analytical replicates, $\delta^{30}\text{Si}$ and $\delta^{29}\text{Si}$, and associated 2 s.d., where analytical replicates are defined as replicate analyses from the same chemical preparation. Averages across chemical preparations within a laboratory group are given by $\delta^{30}\text{Si}$ mean and $\delta^{29}\text{Si}$ mean with associated 2 s.d., 2 s.d. mean. N and n denote the total number of chemical preparations and analytical replicates for each laboratory group. NaN indicates data not available. (b) Measurements of $\delta^{30}\text{Si}(\text{OH})_4$ and $\delta^{29}\text{Si}(\text{OH})_4$ by each laboratory group for ALOHA₃₀₀. The means of analytical replicates, $\delta^{30}\text{Si}$ and $\delta^{29}\text{Si}$, and associated 2 s.d., where analytical replicates are defined as replicate analyses from the same chemical preparation. Averages across chemical preparations within a laboratory group are given by $\delta^{30}\text{Si}$ mean and $\delta^{29}\text{Si}$ mean with associated 2 s.d., 2 s.d. mean. N and n denote the total number of chemical preparations and analytical replicates for each laboratory group. NaN indicates data not available

(a)												
Group ALOHA ₁₀₀₀ m	$\delta^{30}\text{Si}$ [‰]	2 s.d. [‰]	$\delta^{29}\text{Si}$ [‰]	2 s.d. [‰]	^{29/30} Si [‰]	n analyt. replicate	$\delta^{30}\text{Si}$ mean [‰]	2 s.d. mean [‰]	$\delta^{29}\text{Si}$ mean [‰]	2 s.d. mean [‰]	N	n
1	1.15	0.02	0.68	0.07	0.59	1	1.10	0.07	0.63	0.07	4	4
	1.07	0.05	0.62	0.04	0.58	1						
	1.09	0.08	0.61	0.03	0.56	1						
	1.08	0.07	0.61	0.06	0.56	1						
2	1.15	0.01	0.56	0.04	0.49	3	1.10	0.07	0.56	0.02	5	15
	1.09	0.04	0.55	0.01	0.51	2						
	1.07	0.01	0.57	0.05	0.53	3						
	1.07	0.06	0.55	0.03	0.51	4						
3	1.12	0.06	0.57	0.04	0.51	3	1.16	0.16	0.59	0.09	3	9
	1.14	0.08	0.59	0.05	0.52	3						
	1.10	0.00	0.55	0.06	0.50	3						
4	1.25	0.09	0.64	0.08	0.51	3	1.17	0.20	0.62	0.10	3	12
	1.28	0.13	0.66	0.08	0.52	6						
	1.17	0.07	0.62	0.09	0.53	3						
5	1.08	0.13	0.56	0.07	0.52	3	1.23	0.08	0.64	0.04	4	15
	1.19	0.19	0.66	0.10	0.55	5						
	1.20	0.32	0.62	0.07	0.52	3						
	1.27	0.08	0.66	0.04	0.52	3						
6	1.25	0.13	0.62	0.14	0.50	4	1.26	0.12	0.68	0.09	5	5
	1.27	0.10	0.68	0.07	0.53	1						
	1.28	0.11	0.68	0.13	0.53	1						
	1.18	0.23	0.67	0.16	0.57	1						
	1.22	0.22	0.62	0.07	0.51	1						
7	1.33	0.37	0.74	0.12	0.56	1	1.25	0.07	0.65	0.07	6	31
	1.29	0.08	0.70	0.04	0.54	8						
	1.28	0.08	0.62	0.11	0.48	9						
	1.27	0.09	0.66	0.04	0.52	5						
	1.25	0.10	0.65	0.06	0.52	3						
	1.22	0.19	0.66	0.23	0.54	3						
8	1.20	0.17	0.60	0.19	0.50	3	1.29	0.04	0.66	0.02	4	25
	1.27	0.11	0.64	0.06	0.51	12						
	1.29	0.10	0.66	0.05	0.51	6						
	1.27	0.02	0.65	0.01	0.51	2						
	1.31	0.11	0.67	0.06	0.51	5						
9	1.32	0.08	0.69	0.01	0.52	2	1.31	0.15	0.68	0.09	10	20
	1.35	0.07	0.74	0.13	0.55	2						
	1.42	0.16	0.69	0.14	0.49	2						
	1.30	0.11	0.67	0.04	0.51	2						
	1.35	0.21	0.70	0.06	0.52	2						
	1.33	0.01	0.72	0.07	0.54	2						
	1.15	0.07	0.63	0.03	0.55	2						
	1.24	0.07	0.64	0.24	0.51	2						
	1.34	0.11	0.60	0.11	0.45	2						
10	1.31	0.14	0.73	0.10	0.55	2	1.45	0.17	0.76	0.16	3	9
	1.39	0.09	0.70	0.04	0.50	3						
	1.55	0.18	0.85	0.08	0.55	3						
11	1.41	0.12	0.74	0.07	0.52	3	1.27	0.05	0.65	0.03	8	72
	1.26	0.11	0.62	0.08	0.50	9						
	1.25	0.14	0.66	0.07	0.52	9						
	1.23	0.16	0.64	0.08	0.52	9						
	1.27	0.10	0.65	0.12	0.51	9						
	1.30	0.11	0.67	0.08	0.52	9						
	1.28	0.23	0.66	0.09	0.51	9						
	1.30	0.16	0.66	0.09	0.50	9						
1.28	0.16	0.66	0.10	0.52	9							

Table 5 (Contd.)

(b)	$\delta^{30}\text{Si}$ [‰]	2 s.d. [‰]	$\delta^{29}\text{Si}$ [‰]	2 s.d. [‰]	$^{29/30}\text{Si}$	<i>n</i> analyt. replicate	$\delta^{30}\text{Si}$ mean [‰]	2 s.d. mean [‰]	$\delta^{29}\text{Si}$ mean [‰]	2 s.d. mean [‰]	<i>N</i>	<i>n</i>
2	1.75	0.02	0.83	0.03	0.48	2	1.66	0.10	0.84	0.05	6	12
	1.64	0.01	0.87	0.05	0.53	2						
	1.62	0.04	0.86	0.01	0.53	2						
	1.65	0.02	0.81	0.05	0.49	2						
	1.67	0.03	0.81	0.02	0.49	1						
	1.63	0.06	0.85	0.04	0.52	3						
4	1.56	0.06	0.87	0.09	0.55	3	1.64	0.13	0.87	0.05	4	12
	1.60	0.12	0.83	0.02	0.52	3						
	1.66	0.12	0.86	0.01	0.52	3						
	1.71	0.09	0.90	0.03	0.53	3						
5	1.52	0.17	0.76	0.07	0.50	4	1.51	0.12	0.80	0.08	3	11
	1.56	0.18	0.84	0.14	0.53	4						
	1.45	0.08	0.81	0.05	0.56	3						
6	1.95	0.37	0.98	0.19	0.50	1	1.78	0.18	0.89	0.18	6	6
	1.76	0.27	0.90	0.17	0.51	1						
	1.76	0.30	0.86	0.19	0.49	1						
	1.75	0.07	0.74	0.16	0.42	1						
	1.68	0.37	0.98	0.12	0.58	1						
	1.81	0.38	0.91	0.22	0.50	1						
7	1.92	0.13	0.98	0.05	0.51	2	1.92	0.08	1.02	0.12	5	14
	1.97	0.02	1.05	0.11	0.53	3						
	1.95	0.08	1.07	0.01	0.55	3						
	1.87	0.30	0.94	0.32	0.50	3						
	1.89	0.07	1.07	0.08	0.57	3						
8	1.51	0.05	0.77	0.05	0.51	3	1.46	0.17	0.75	0.09	3	10
	1.52	0.04	0.77	0.02	0.51	1						
	1.36	0.09	0.69	0.04	0.51	6						
9	1.90	0.01	0.95	0.06	0.50	2	1.94	0.12	0.99	0.08	8	16
	2.05	0.16	1.06	0.08	0.52	2						
	1.90	0.57	0.98	0.21	0.51	2						
	1.94	0.01	0.94	0.10	0.48	2						
	2.02	0.42	1.04	0.11	0.51	2						
	1.91	0.10	1.00	0.24	0.52	2						
	1.89	0.27	0.99	0.14	0.53	2						
	1.95	0.27	1.01	0.10	0.52	2						
10	1.52	0.04	0.77	0.02	0.51	3	1.53	0.17	0.79	0.06	3	9
	1.45	0.05	0.77	0.02	0.53	3						
	1.61	0.07	0.82	0.06	0.51	3						
11	1.61	NaN	0.88	NaN	0.55	1	1.69	0.24	0.85	0.17	8	8
	1.82	NaN	0.97	NaN	0.54	1						
	1.73	NaN	0.90	NaN	0.52	1						
	1.52	NaN	0.71	NaN	0.46	1						
	1.60	NaN	0.77	NaN	0.48	1						
	1.76	NaN	0.91	NaN	0.52	1						
	1.86	NaN	0.85	NaN	0.46	1						
	1.61	NaN	0.80	NaN	0.50	1						

One laboratory (group 1) treated samples with ultraviolet light/ozone to remove dissolved organic carbon (DOC; Table 1) as Hughes *et al.*³⁷ found significant biases in $\delta^{30}\text{Si}$ data when DOC concentrations significantly exceeded those of dissolved Si.

3 Results

The seawater samples collected from 300 m (300.21 decibar pressure, 13.37 °C, salinity 34.311) and 1000 m (1021.65 decibar pressure, 3.88 °C, salinity 34.467) at Station ALOHA resulted in

the desired range of $\text{Si}(\text{OH})_4$ concentrations with measured concentrations of $9.18 \pm 0.05 \mu\text{mol L}^{-1}$ and $112.8 \pm 0.5 \mu\text{mol L}^{-1}$ for ALOHA₃₀₀ and ALOHA₁₀₀₀, respectively.

In total, 11 laboratory groups participated in the seawater inter-calibration study. The $\delta^{30}\text{Si}(\text{OH})_4$ values for ALOHA₃₀₀ and ALOHA₁₀₀₀ from each laboratory were in good overall agreement. Average values from individual laboratories for ALOHA₃₀₀ ranged from +1.46‰ to +1.94‰, with a mean value of $+1.68 \pm 0.35\text{‰}$ (2 s.d., results from 9 groups). $\delta^{30}\text{Si}(\text{OH})_4$ values for ALOHA₁₀₀₀ ranged between +1.10‰ and +1.45‰ with a mean of

+1.24 ± 0.20‰ (2 s.d., results from 11 groups; Fig. 1, Table 2). Normal probability plots of the laboratory group means for each sample were highly linear with $R^2 \geq 0.95$ (Fig. 2). Shapiro's tests confirmed that the group averages for ALOHA₃₀₀ were normally distributed ($W = 0.966$, $p = 0.21$, where H_0 is that the data are from a normal distribution); however, group means for ALOHA₁₀₀₀ were not ($W = 0.954$, $p = 0.036$). In the latter case the median or modal value may be better measures of central tendency. Median values and interquartile deviations, *i.e.* 0.5 × (75% quartile – 25% quartile), for ALOHA₃₀₀ and ALOHA₁₀₀₀, are +1.66 ± 0.13‰ and +1.25 ± 0.06‰ respectively (Table 2) with corresponding modal values of 1.66‰ and 1.22‰. Values obtained for Big Batch and Diatomite by each group that measured these materials (Table 6) were within the uncertainty bounds of the values established by Reynolds *et al.*¹⁷

The reproducibility of measurements for the seawater samples within individual groups ranged from 0.04‰ to 0.24‰ for the standard deviations and 0.06‰ to 0.13‰ for the interquartile deviations with the larger variation generally obtained for ALOHA₃₀₀ (Fig. 1, Table 2). For each sample testing for statistically significant differences in the mean isotope values obtained by each group is confounded as all groups used a single mass spectrometer type negating the use of a two-way ANOVA to simultaneously test for differences among groups and among mass spectrometer types. Testing for differences in the mean isotope values across groups was thus restricted to tests among laboratories using the same mass spectrometer type. Tests for differences among sample preparations methods reveal no significant sample preparation effect (see below) so the effect of preparation was subsumed in the mean square error when examining differences among laboratory groups.

Considering groups that used a Neptune mass spectrometer the ANOVA revealed significant differences among mean values

across groups for ALOHA₁₀₀₀ ($F = 27.2$, d.f. = 3, $p < 0.001$), but not for ALOHA₃₀₀ ($F = 0.30$, d.f. = 1, $p = 0.59$, note only two groups measured ALOHA₃₀₀ using a Neptune) indicating the presence of small, but statistically significant, biases between laboratories for ALOHA₁₀₀₀. However, Levene's test showed unequal variances across groups for both ALOHA₃₀₀ ($F = 8.85$, d.f. = 1, $p = 0.012$) and for ALOHA₁₀₀₀ ($F = 3.35$, d.f. = 3, $p = 0.045$) so that the results of the ANOVA should be interpreted with caution. When these data were re-evaluated using Welch's ANOVA the presence of significant differences among means for ALOHA₁₀₀₀ ($F = 38.2$, d.f. = 3, $p < 0.0004$) and the lack of any significant differences among groups for ALOHA₃₀₀ ($F = 0.374$, d.f. = 1, $p = 0.55$) were confirmed. *Post hoc* tests (Table 7) revealed that differences among laboratories were not consistent between the two seawater samples.

A similar analysis investigating differences among groups using Nu Plasma mass spectrometers showed significant differences among means for both ALOHA₃₀₀ ($F = 34.5$, d.f. = 5, $p < 0.001$) and ALOHA₁₀₀₀ ($F = 6.90$, d.f. = 5, $p = 0.0004$). In both cases the assumption of equality of variances was met (Levine: $F = 0.765$, d.f. = 5, $p = 0.58$ and $F = 0.421$, d.f. = 5, $p = 0.83$ for ALOHA₁₀₀₀ and ALOHA₃₀₀, respectively). Similar to the case for the Neptune, *post hoc* tests (Table 8) showed that the pattern of significant differences among group means for the Nu Plasma shifted between ALOHA₃₀₀ and ALOHA₁₀₀₀. The shifting biases among groups seen for both instruments is also seen in the change in rank order of the mean isotope values obtained by each group between the ALOHA₁₀₀₀ and ALOHA₃₀₀ samples (Fig. 1).

An indicator for the quality of $\delta^{30}\text{Si}$ measurements is given by the slope of the relationship between $\delta^{30}\text{Si}$ and $\delta^{29}\text{Si}$ values, as any polyatomic interferences during MC-ICP-MS measurements would lead to an offset from predicted equilibrium or kinetic fractionation line. Least squares linear regression between $\delta^{30}\text{Si}(\text{OH})_4$ and $\delta^{29}\text{Si}(\text{OH})_4$ produces a slope of 0.5188 ± 0.0184 (s.e., $R^2 = 0.98$; Fig. 3). Repeating the analysis using reduced major axis model II regression that gives equal weight to errors in both $\delta^{29}\text{Si}(\text{OH})_4$ and $\delta^{30}\text{Si}(\text{OH})_4$ yields a slope of 0.5131 ± 0.0040 (s.e., $R^2 = 0.98$).

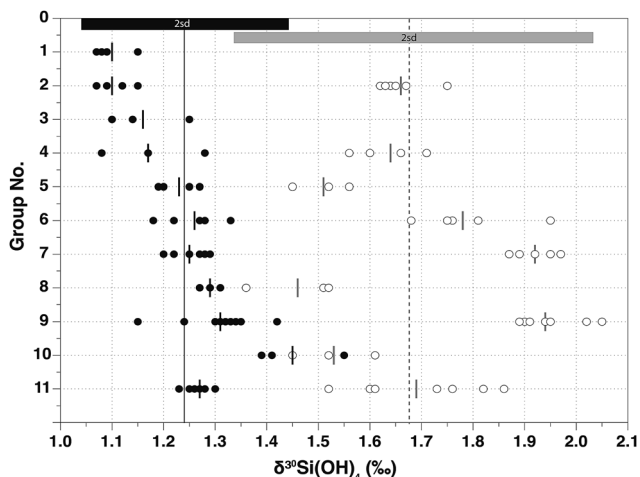


Fig. 1 $\delta^{30}\text{Si}(\text{OH})_4$ results from all groups for ALOHA₃₀₀ (open circles) and ALOHA₁₀₀₀ (filled circles). The long black vertical solid line indicates the mean value of all measurements for ALOHA₁₀₀₀ and the long dashed line that for ALOHA₃₀₀. The data points represent the individual $\delta^{30}\text{Si}(\text{OH})_4$ values from Table 5. Short vertical solid lines are the means obtained by individual laboratories for the two samples. Uncertainty in the mean for all measurements for each sample (2 s.d.) is indicated by the horizontal bars at the top of the figure.

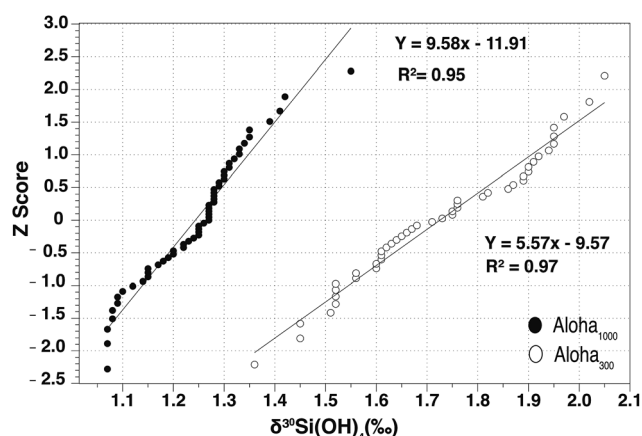


Fig. 2 Z scores as a function of $\delta^{30}\text{Si}(\text{OH})_4$ for ALOHA₃₀₀ (open circles) and ALOHA₁₀₀₀ (filled circles).

Table 6 Summary of mean Si isotope values ($\delta^{30}\text{Si}$, $\delta^{29}\text{Si}$), the associated 2σ analytical uncertainty (2 s.d.) and the number of measurements (n) obtained by each laboratory group for the secondary standards Big Batch and Diatomite. The overall mean and the uncertainty about the mean (2 s.d.) as well as the median and the interquartile deviation (IQD) for all groups are given at the bottom of the table. NaN indicates data not available

Group	Big Batch					Diatomite				
	$\delta^{30}\text{Si}$	2 s.d.	$\delta^{29}\text{Si}$	2 s.d.	n	$\delta^{30}\text{Si}$	2 s.d.	$\delta^{29}\text{Si}$	2 s.d.	n
1	-10.61	0.08	-5.42	0.07	18	1.25	0.11	0.64	0.09	15
2	NaN	NaN	NaN	NaN	NaN	1.26	0.14	0.66	0.12	14
3	-10.48	0.34	NaN	NaN	3	NaN	NaN	NaN	NaN	NaN
4	NaN	NaN	NaN	NaN	NaN	1.25	0.13	NaN	NaN	19
5	-10.67	0.16	-5.43	0.10	5	1.23	0.05	0.63	0.04	4
6	-10.64	0.22	-5.43	0.10	34	NaN	NaN	NaN	NaN	NaN
7	-10.50	0.08	-5.36	0.06	3	NaN	NaN	NaN	NaN	NaN
8	-10.51	0.23	-5.35	0.11	25	1.27	0.16	0.66	0.07	5
9	-10.48	0.08	NaN	NaN	2	NaN	NaN	NaN	NaN	NaN
10	NaN	NaN	NaN	NaN	NaN	NaN	NaN	NaN	NaN	NaN
11	NaN	NaN	NaN	NaN	NaN	NaN	NaN	NaN	NaN	NaN
Mean	-10.56		-5.40			1.25		0.65		
2 s.d.	0.16		0.08			0.03		0.03		
Median	-10.51		-5.42			1.25		0.65		
IQD	0.07		0.04			0.01		0.01		

Table 7 Statistical analysis of differences in differences in $\delta^{30}\text{Si}(\text{OH})_4$ among groups using Neptune spectrometers. Groups not connected by same letter are significantly different

Group	Tukey		False discovery rate		Mean $\delta^{30}\text{Si}(\text{OH})_4$
	Column A	Column B	Column A	Column B	
ALOHA₁₀₀₀					
11	A		A		1.27
2		B	A	B	1.16
3		B		B	1.10
1		B		B	1.10
ALOHA₃₀₀					
11	A				1.69
2	A				1.66

Table 8 Statistical analysis of differences in differences in $\delta^{30}\text{Si}(\text{OH})_4$ among groups using Nu Plasma mass spectrometers. Groups not connected by same letter are significantly different

Group	Tukey			Mean $\delta^{30}\text{Si}(\text{OH})_4$
	Column A	Column B	Column C	
ALOHA₁₀₀₀				
10	A			1.45
9		B		1.31
6		B	C	1.26
7		B	C	1.25
5		B	C	1.23
4			C	1.18
ALOHA₃₀₀				
9	A			1.94
7	A			1.92
6		B		1.78
4			C	1.64
10			C	1.53
5			C	1.51

Fig. 4 shows the $\delta^{30}\text{Si}(\text{OH})_4$ data for all measurements grouped by mass spectrometer type (Fig. 4a and b) and by co-precipitation method (Fig. 4c and d). Considering mass spectrometer types the Neptune and Nu Plasma types are replicated across groups while the IRMS is not as IRMS was used by a single group. Thus statistical analysis of mass spectrometer type was only possible for Neptune and Nu Plasma types. Furthermore, as each laboratory used a single mass spectrometer the data from the same group are not independent. To account for this lack of independence an ANOVA with Neptune

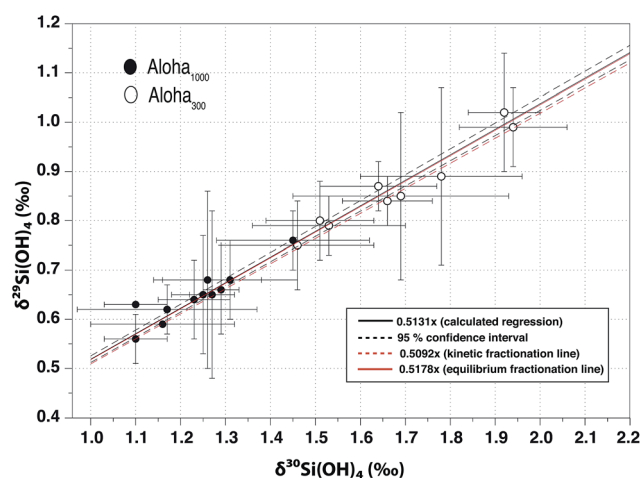


Fig. 3 Plot of $\delta^{30}\text{Si}(\text{OH})_4$ versus $\delta^{29}\text{Si}(\text{OH})_4$ for ALOHA₃₀₀ (open circle) and ALOHA₁₀₀₀ (filled circle; error bars are 2 s.d.). Solid line is the result of least-squares linear regression with a slope of 0.5188 ± 0.0184 (s.e., $R^2 = 0.98$). The lower and upper 95% confidence intervals are given as dashed black lines. The kinetic fractionation line has a slope of 0.5092 (intercept of zero) for Si (dashed red line) and the equilibrium fractionation line has a slope of 0.5178 (intercept of zero) for Si (solid red line). Regression line obtained by analysis using reduced major axis model II regression yields a slope of 0.5131 ± 0.0040 (s.e., $R^2 = 0.98$; not displayed in the figure).

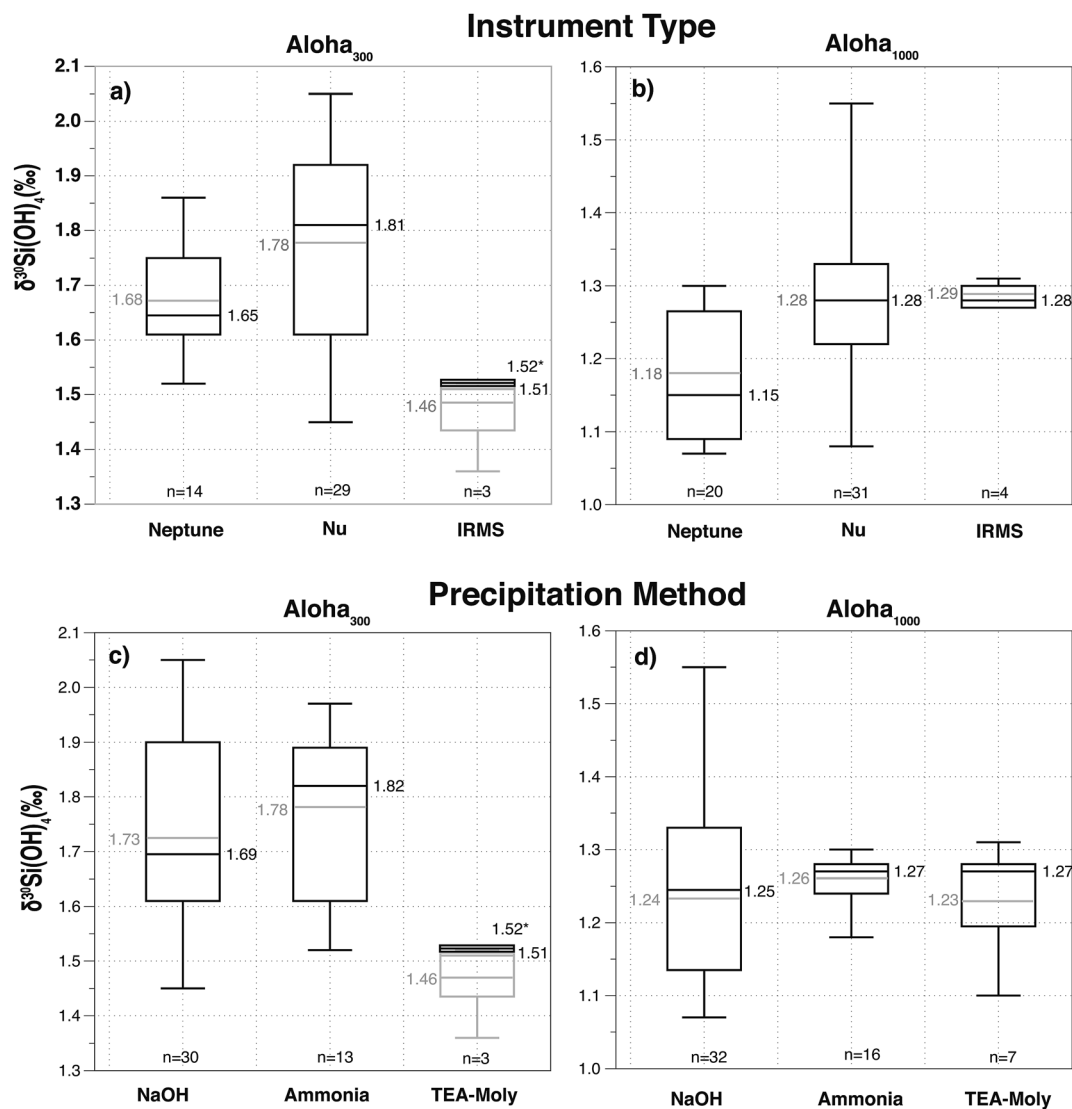


Fig. 4 Boxplots showing $\delta^{30}\text{Si}(\text{OH})_4$ data sorted by different mass spectrometer types for (a) ALOHA₃₀₀ and for (b) ALOHA₁₀₀₀. Data sorted by different precipitation methods for (c) ALOHA₃₀₀ and (d) ALOHA₁₀₀₀. On the boxplots the median values (black) and the mean values (grey) are displayed. For ALOHA₃₀₀ (a) and (c) show data for IRMS and TEA-moly with (grey boxplot) and without outlier (black boxplot). Here, the mean value (which equals the median) is indicated by a superscript star. The value next to each boxplot indicates the median (black) and the mean (grey), respectively. The number of included data points (*n*) is given below each boxplot. Raw data are presented in Table 3.

and Nu Plasma as main effects was performed on the average values obtained by each group weighted by the number of measurements contributing to each mean. Those results show no significant differences between the results obtained on the Neptune *versus* the Nu Plasma for ALOHA₃₀₀ ($F = 0.687$, d.f. = 1, $p = 0.44$) and likewise for ALOHA₁₀₀₀ ($F = 3.75$, d.f. = 1, $p = 0.089$). In qualitative terms the values obtained by IRMS are nearly identical to those obtained using the Nu Plasma for ALOHA₁₀₀₀, but they appear lower than the averages for either the Nu Plasma or Neptune for ALOHA₃₀₀. That difference is driven by one low value of +1.36‰ measured by IRMS (Table 5). If that value is considered an outlier the resulting mean for IRMS becomes closer to that for the other two mass spectrometer types, +1.52‰ (Fig. 4).

ANOVAs evaluating the effect of different precipitation methods showed no differences among NaOH, ammonia or

TEA-moly procedures for ALOHA₁₀₀₀ ($F = 0.27$, d.f. = 2, $p = 0.77$), but a significant difference for ALOHA₃₀₀ ($F = 4.7$, d.f. = 2, $p = 0.014$) driven by a lower mean value for TEA-moly precipitation compared to the other two methods (Table 3, Fig. 4). For ALOHA₃₀₀ the significant differences between precipitation methods are driven by one outlier value mentioned above (Table 5). When that value is removed from the analysis no significant differences among precipitation methods ($F = 2.4$, d.f. = 2, $p = 0.10$) are found for ALOHA₃₀₀. We are quick to point out that the ANOVA used to detect differences among precipitation methods necessarily incorporated the effects of groups and of mass spectrometer type into the mean square error as the experimental design is confounded so that these results should be viewed with caution. One group, group 6, utilized both NaOH and ammonia co-precipitation methods allowing a direct comparison of methods for this one group. Here too there was

no significant difference between precipitation methods ($F = 0.61$, d.f. = 1, $p = 0.49$).

4 Discussion

4.1 General results

We present the first inter-laboratory study comparing the stable silicon isotope composition of dissolved $\text{Si}(\text{OH})_4$ in seawater. Samples with both a relatively low and a relatively high $\text{Si}(\text{OH})_4$ concentration were used to evaluate the influence of varying degrees of Si pre-concentration and varying matrix to analyte ratios. The results from the 11 laboratories were in good agreement for both samples, despite the use of different sample preparation and purification methods and different mass spectrometer models (Nu Plasma *versus* Neptune) and types (MC-ICP-MS *versus* IRMS). The mean $\delta^{30}\text{Si}(\text{OH})_4$ values for ALOHA₃₀₀ and ALOHA₁₀₀₀ were $+1.68 \pm 0.35\%$ and $+1.24 \pm 0.20\%$ (2 s.d.), respectively (Fig. 1, Table 2). Given that the data for ALOHA₁₀₀₀ are not normally distributed a better representation of the central tendency is the median. Median values and interquartile deviations for ALOHA₃₀₀ and ALOHA₁₀₀₀, are $+1.66 \pm 0.13\%$ and $+1.25 \pm 0.06\%$ respectively (Table 2). Modal values are nearly identical (within 0.03%) of corresponding median values (Table 2).

The slope of the least squares fit of $\delta^{30}\text{Si}(\text{OH})_4$ *versus* $\delta^{29}\text{Si}(\text{OH})_4$ relationship, 0.5188 is statistically indistinguishable from the theoretical value of 0.5178 for equilibrium control of fractionation^{38,39} ($t = 0.302$, d.f. = 19, $p = 0.38$) and significantly higher than those for kinetic fractionation, *i.e.* 0.5047 or 0.5092 depending on whether elemental Si or SiO_2 is fractionating, respectively³⁹ ($t = 4.26$, d.f. = 19, $p < 0.0001$ for Si and $t = 2.90$, d.f. = 19, $p < 0.0001$ for SiO_2). The slope of the reduced major axis regression, 0.5131, is statistically indistinguishable from both the theoretical value for equilibrium fraction ($t = 1.17$, d.f. = 19, $p = 0.13$) and the kinetic fractionation of SiO_2 ($t = 0.94$, d.f. = 19, $p = 0.97$), but it was statistically larger than the theoretical value for the kinetic fractionation of elemental Si ($t = 2.10$, d.f. = 19, $p < 0.00001$). For reference the Bonferroni corrected p value for these six comparisons is 0.008. Thus, the data lack the precision necessary to discriminate between control by equilibrium or kinetic fractionation. Ultimately, the fractionation of $\text{Si}(\text{OH})_4$ in the sea should be kinetically controlled given the strong role of biology in the process.⁴⁰

The tight relationship between $\delta^{30}\text{Si}(\text{OH})_4$ and $\delta^{29}\text{Si}(\text{OH})_4$ relationship does indicate insignificant isobaric interference problems during Si isotope analysis. External reproducibility (2 s.d.) during this study (0.20% and 0.35% for ALOHA₁₀₀₀ and ALOHA₃₀₀, respectively) were similar to those obtained during the inter-laboratory comparison of Si isotopes in pure siliceous solid materials,¹⁷ where 2 s.d. uncertainty values of 0.22%, 0.16% and 0.54% were obtained for the standards IRMM-018, Diatomite and Big Batch, respectively. Analyzing both ALOHA₃₀₀ and ALOHA₁₀₀₀ as a routine part of future studies of seawater Si isotopes will allow potential biases to be quantified, facilitating comparisons among data sets.

The suite of methodologies used to analyze the isotopic composition of Si in the seawater samples all yielded robust results. Comparison of the data obtained from the low and high

concentration samples suggests that further improvement may be possible. Overall ALOHA₁₀₀₀ shows a better reproducibility ($\pm 0.20\%$ s.d., 0.05% i.q.d) than ALOHA₃₀₀ ($\pm 0.35\%$ s.d., 0.13% i.q.d.) among laboratories and within each laboratory (Fig. 1, Table 2). Small, but statistically significant, differences in the mean isotope values among laboratories were detected for both samples (Table 7). Moreover, the number and magnitude of significant differences changed between the low and high concentration samples (Table 7). Together these results imply that differences in how the two samples were processed marginally influenced the results.

The main difference in sample preparation between ALOHA₃₀₀ and ALOHA₁₀₀₀ was the larger sample volume processed for ALOHA₃₀₀ (Table 4). The volume of seawater used for pre-concentration scales inversely with the $\text{Si}(\text{OH})_4$ concentration in the sample such that larger volumes are processed for samples with low Si concentration. To the extent that they are not removed during the chromatographic purification of Si, the carryover of seawater ions (*e.g.* Mg^{2+} , Na^+ , Ba^{2+} , Cl^- , SO_4^{2-}) will be a function of the sample volume processed, altering the ratio of these ions to the analyte Si in the final sample which may produce matrix effects during measurements (see Methods). As most groups use a cation exchange resin as the final purification step (Table 1), residual anions are likely present.

Another possible cause of the larger variance of the measurements of ALOHA₃₀₀ could be the higher DOC to Si ratio in the shallow sample. Any element remaining in the solution analyzed can compete with analyte for ionization within the plasma and thus can potentially induce a matrix effect on isotopic mass bias. Hughes *et al.*³⁷ (2011) showed that a DOC : Si mass ratio (as C : Si) above 0.6 can interfere with $\delta^{30}\text{Si}$ measurements. DOC concentrations measured on the same cruise and at the same depths as sampled for Si isotopes were 48 and 37 $\mu\text{mol C L}^{-1}$ for ALOHA₃₀₀ and ALOHA₁₀₀₀, respectively (C. A. Carlson, pers. com.), which are three orders of magnitude lower than in the samples analyzed by Hughes *et al.*³⁷ However, DOC/Si mass ratios (C/Si) were 2.2 and 0.1 for ALOHA₃₀₀ and ALOHA₁₀₀₀, respectively. Those ratios imply a potential for interference from DOC in ALOHA₃₀₀ if DOC is concentrated at the same efficiency as Si during the sample pre-concentration procedure. Detailed investigations into these and other possible interferences may improve the analytical precision obtained for low concentration samples.

4.2 Potential instrument biases

Measurements on the Neptune (mean = $+1.18 \pm 0.18\%$) and the Nu Plasma (mean = $+1.28 \pm 0.18\%$) show a slight and only marginally significant ($p = 0.089$) offset for ALOHA₁₀₀₀ with the values from the Neptune being lower by 0.1%. For ALOHA₃₀₀ the mean value on the Neptune is also lower than on the Nu Plasma by 0.1% (Table 3), but in this case the difference is far from statistically significant given the larger variance of the measurements for the shallow sample. One possible explanation for this offset could be the applied Mg doping of the sample, which is mainly conducted for measurements on the Neptune (except for group 11), to correct for the instrumental mass bias.²¹ This possibility was investigated by examining the

results for group 11, which performed Si isotope analysis on a Neptune without Mg doping. The mean value for this group was slightly higher $+1.27 \pm 0.05\%$ (2 s.d.), than the Neptune mean. Only one group (group 10) applied Mg doping using a Nu Plasma, which resulted in a mean value of $+1.45 \pm 0.17\%$, higher than the average $\delta^{30}\text{Si}$ value of $+1.28 \pm 0.18\%$ obtained by groups using the Nu Plasma without Mg doping. The results are thus inconclusive, and it is not clear whether Mg doping or an instrument bias caused the small offset between the results from the Neptune and Nu Plasma instruments.

The average $\delta^{30}\text{Si}(\text{OH})_4$ value from IRMS match the average from the Nu Plasma for ALOHA₁₀₀₀, but they are lower than both the Nu Plasma or Neptune data for ALOHA₃₀₀. It is difficult to draw firm conclusions from these similarities and differences given the very large difference in the volume of seawater processed for measurement by IRMS compared to the other instrument types (Table 3).

4.3 Possible improvement of chemical preparation and $\delta^{30}\text{Si}$ measurements

There are several approaches to reduce “matrix effects” in MC-ICP-MS measurements caused by remnants of DOC and seawater ions in samples.^{37,41} Methods that further reduce the ion concentrations (cations and anions) may thus be beneficial or ion concentrations in the sample solution could be measured and the samples doped prior to measurement, though the latter may be cumbersome for studies with large numbers of samples. Alternatively, a sequential cation–anion-exchange chromatography purification procedure, such as has been tested by some groups for $\delta^{30}\text{Si}(\text{OH})_4$ (N. Estrade, pers. comm.), may be a promising approach. Closset *et al.*⁴² showed that the contribution of Cl^- originating from seawater can be neglected when HCl is used to dissolve the brucite produced during Mg co-precipitation as the Cl^- from the acid is present in large excess (up to 0.5 mol L^{-1}) compared to remaining Cl^- from seawater. Similarly, the occurrence of NO_3^- in seawater is negligible when HNO_3 (0.5 mol L^{-1}) is used as a solvent in both the samples and standards. In the present study group 2 employed a mixture that was 0.5 mol L^{-1} HCl, 0.5 mol L^{-1} HNO_3 and 1 mmol L^{-1} H_2SO_4 to simultaneously compensate for the presence of Cl^- , NO_3^- and SO_4^{2-} .

The concentration of SO_4^{2-} ions remaining after chemical purification of the Si (*i.e.* not collected by cation exchange resin) depends on the volume of seawater used for the NaOH and ammonia methods. There is, however, no simple relationship between total sample volume processed and final SO_4^{2-} concentration, since most seawater is discarded during the pre-concentration procedure. Some laboratories also observed that the presence of high SO_4^{2-} (higher than 0.5 mmol L^{-1}) may cause a negative shift in the baseline of ^{29}Si and ^{30}Si due to the high ^{32}S signal. More importantly, this impact will directly alter the Si^+ signal intensity and is different from the matrix effect, and cannot be corrected using the matrix-match approach (Zhang A., data unpublished). The influence of residual ions also varies with the number of co-precipitations employed as the two-step NaOH process developed by Reynolds *et al.*⁷ significantly reduces the final seawater volume from which Si is stripped compared to

a one step co-precipitation. Furthermore, a general treatment of seawater sample with ultra violet light, ozone or peroxide to reduce the influence of dissolved organic matter, as already suggested by Hughes *et al.*³⁷ may be beneficial.

The IRMS method is largely free of “matrix effects”. Interference from SiOF_2 is rare as a significant signal at m/z 83 that would indicate the presences of the compound (see above) are rarely observed. The major challenge with the Cs_2SiF_6 IRMS method is the large sample size required compared to MC-ICP-MS. When less than $5 \mu\text{moles}$ of Cs_2SiF_6 are analyzed the resulting $\delta^{30}\text{Si}$ values are significantly biased to higher values.¹⁹ This is not a limitation of the instrument, as the Kiel III/MAT 252 combination is capable of analyzing at least an order of magnitude lower amount of Si. The reason for the apparent fractionation of small samples is unknown. Overcoming this limitation would allow seawater sample volumes similar to those currently employed for MC-ICP-MS analysis. The lower limit of sample size would then essentially only be determined by the mass of Si necessary to quantitatively precipitate Cs_2SiF_6 .

4.4 Best practices during MC-ICP-MS measurements

The major challenges during MC-ICP-MS measurements leading to lower accuracy and precision are (i) molecular interference at m/z ^{28}Si ($^{14}\text{N}_2$, $^{12}\text{C}^{16}\text{O}$), ^{29}Si ($^{14}\text{N}_2^1\text{H}$, $^{12}\text{C}^1\text{H}^{16}\text{O}^{15}\text{N}^{14}\text{N}$) and ^{30}Si ($^{14}\text{N}^{16}\text{O}$) and (ii) variable mass-dependent fractionation in the instrument (mass-bias, see also Cardinal *et al.*²¹). To handle possible problems with interfering compounds the matrix blank should not exceed 1% of the sample sensitivity and it should be routinely measured and subtracted from the measurement signal. Furthermore the achieved resolving power (10% peak valley definition) of the mass spectrometer should be above 3500 in order to clearly separate molecular interference masses. All of these issues are also influenced by operating condition (“plasma conditions”), non-analyte composition of the particular sample (“matrix effect”) and the amount of material that is introduced into the instrument (“mass-load effect”), which is determined by the Si concentration introduced into the instrument by the sample gas flow. A study by Zhang *et al.*²³ also demonstrated that the sample gas flow has an effect on the production of polyatomic ions besides its obvious effects on sensitivity and stability. The importance of the energetic/thermal “plasma conditions” during ICP-MS measurements for precise and accurate stable isotope measurements was recently shown.⁴³ Therefore, in addition to the elemental purity of the sample and the Si concentration introduced into the instrument, plasma conditions should be monitored carefully in order to improve the accuracy and precision of $\delta^{30}\text{Si}$ measurements. This may require allowing the instrument to stabilize for several hours before measurements.

4.5 Recommendations

The inter-calibration results show a very good precision within all participating groups taking into account the external reproducibility of the individual measurements. However, small but statistically significant differences among mean values across groups were observed for both samples. Such differences can be rigorously quantified through routine analysis of these

reference waters as part of future studies of $\delta^{30}\text{Si}(\text{OH})_4$ distributions in the ocean. This is particularly important for international programs such as GEOTRACES for which global data from multiple laboratories are often combined for analysis. It is recommended that future studies analyzing $\delta^{30}\text{Si}(\text{OH})_4$ in seawater also analyze ALOHA₃₀₀ and ALOHA₁₀₀₀ and report these results to facilitate and evaluate comparability of data between laboratories. While the use of ALOHA samples is needed to validate the seawater processing procedures, analytical conditions and instrument stability should first be checked for each analytical session by measuring secondary reference materials such as Diatomite and Big Batch which are more readily available.¹⁷ ALOHA samples, Diatomite and Big Batch can be obtained from Mark Brzezinski at UCSB. Finally, a plan for reference water renewal must be developed to facilitate inter-calibration efforts in the future.

Acknowledgements

Our thanks to Matthew Church for his help in obtaining seawater samples from Hawaii Ocean Time Series station ALOHA. This work was supported by OCE-1233029 from the US National Science Foundation, Chemical Oceanography Program to MB. DC thanks for their financial support the EU FP7 (CIG #294146) and IPSL. GFDS is funded by a Marie Skłodowska-Curie Research Fellowship under EU Horizon2020 (SOSiC, GA #708407). PG and MF acknowledge funding by the Collaborative Research Centre 754 “Climate-Biogeochemistry interactions in the Tropical Ocean” (www.sfb754.de), supported by the Deutsche Forschungsgemeinschaft (DFG). The work by JNS was supported by the “Laboratoire d'Excellence” LabexMER (ANR-10-LABX-19) and co-funded by a grant from the French government under the program “Investissements d'Avenir”, and by a grant from the Regional Council of Brittany (SAD programme). AZ and JZ were supported by the Ministry of Science and Technology of China (grant 2011CB409801). QL and DL acknowledge financial support from the National Natural Science Foundation of China (No. 21422509 and 91543104). RF and DW acknowledge financial support from the Natural Sciences and Engineering Research Council of Canada and NE benefitted from a post-doctoral fellowship from NSERC (CREATE – MAGNET). CE and KP acknowledge the funding from ICBM (Univ. of Oldenburg) and the Max Planck Institute for Marine Microbiology Bremen. PA, EK and MS acknowledge the financial support of Vetenskapsrådet, Sweden, for funding the Vegacenter at NRM Stockholm (grant #829-2011-6326). We also would like to acknowledge William Rice and Wilfried Rickels for the improvement of the statistics.

References

- 1 P. J. Tréguer and C. L. De La Rocha, *Annual Review of Marine Science*, 2013, **5**, 477–501.
- 2 B. C. Reynolds, M. Frank and A. N. Halliday, *Paleoceanography*, 2008, **23**, PA4219.
- 3 E. Maier, B. Chaplignin, A. Abelmann, R. Gersonde, O. Esper, J. Ren, H. Friedrichsen, H. Meyer and R. Tiedemann, *Journal of Quaternary Science*, 2013, **28**, 571–581.
- 4 C. Ehlert, P. Grasse, D. Guitierrez, R. Salvatelli and M. Frank, *Climate of the Past*, 2015, **11**, 1–16.
- 5 C. De La Rocha, M. A. Brzezinski and M. J. DeNiro, *Geochim. Cosmochim. Acta*, 2000, **64**, 2467–2477.
- 6 D. Cardinal, L. Y. Alleman, F. Dehairs, N. Savoye, T. W. Trull and L. André, *Global Biogeochem. Cycles*, 2005, **19**, GB2007.
- 7 B. Reynolds, M. Frank and A. Halliday, *Earth Planet. Sci. Lett.*, 2006, **244**, 431–443.
- 8 Z. Cao, M. Frank and M. Dai, *Limnol. Oceanogr.*, 2015, **60**, 1619–1633.
- 9 G. F. de Souza, B. C. Reynolds, G. C. Johnson, J. L. Bullister and B. Bourdon, *Biogeosciences*, 2012, **9**, 4199–4213.
- 10 M. A. Brzezinski and J. L. Jones, *Deep Sea Res., Part II*, 2015, **116**, 79–88.
- 11 S. P. Singh, S. K. Singh, R. Bhushan and V. K. Rai, *Geochim. Cosmochim. Acta*, 2015, **151**, 172–191.
- 12 A. Y. Zhang, J. Zhang, J. Hu, R. F. Zhang and G. S. Zhang, *J. Geophys. Res.: Oceans*, 2015, **120**, 6943–6957.
- 13 G. F. de Souza, R. D. Slater, J. P. Dunne and J. L. Sarmiento, *Earth Planet. Sci. Lett.*, 2014, **398**, 66–76.
- 14 G. F. de Souza, R. D. Slater, M. P. Hain, M. A. Brzezinski and J. L. Sarmiento, *Earth Planet. Sci. Lett.*, 2015, **432**, 342–353.
- 15 M. Holzer and M. A. Brzezinski, *Global Biogeochem. Cycles*, 2015, **29**, 267–287.
- 16 S. Gao, D. A. Wolf Gladrow and C. Völker, *Global Biogeochem. Cycles*, 2016, **30**, 120–133, DOI: 10.1002/2015GB005189.
- 17 B. C. Reynolds, J. Aggarwal, L. André, D. Baxter, C. Beucher, M. A. Brzezinski, E. Engström, R. Bastan Georg, M. Land, M. J. Leng, S. Opfergelt, I. Rodushkin, H. J. Sloane, S. H. J. M. van den Boorn, P. Z. Vroon and D. Cardinal, *J. Anal. At. Spectrom.*, 2007, **22**, 561–568.
- 18 C. De La Rocha, M. A. Brzezinski and M. J. DeNiro, *Anal. Chem.*, 1996, **68**, 3746–3750.
- 19 M. A. Brzezinski, J. L. Jones, C. P. C. Beucher, M. S. M. Demarest and H. L. H. Berg, *Anal. Chem.*, 2006, **78**, 6109–6114.
- 20 C. L. De La Rocha, *Geochem., Geophys., Geosyst.*, 2002, **3**, DOI: 10.1029/2002GC000310.
- 21 D. Cardinal, L. Y. Alleman, J. De Jong, K. Ziegler and L. André, *J. Anal. At. Spectrom.*, 2003, **18**, 213–218.
- 22 C. L. De La Rocha, P. Bescont, A. Croguennoc and E. Ponzevera, *Geochim. Cosmochim. Acta*, 2011, **75**, 5283–5295.
- 23 A. Zhang, J. Zhang, R. Zhang and Y. Xue, *Chin. J. Anal. Chem.*, 2015, **43**, 1353–1359.
- 24 P. Grasse, C. Ehlert and M. Frank, *Earth Planet. Sci. Lett.*, 2013, **380**, 60–71.
- 25 C. P. Beucher, M. A. Brzezinski and J. L. Jones, *Geochim. Cosmochim. Acta*, 2008, **72**, 3063–3073.
- 26 H. J. M. van den Boorn, P. Z. Vroon and M. J. Bergen, *J. Anal. At. Spectrom.*, 2009, **24**, 1111–1114, DOI: 10.1039/b816804k.
- 27 G. F. de Souza, B. C. Reynolds, J. Rickli, M. Frank, M. A. Saito, L. J. A. Gerringa and B. Bourdon, *Global Biogeochem. Cycles*, 2012, **26**, GB2035.
- 28 R. Georg, B. Reynolds, M. Frank and A. Halliday, *Chem. Geol.*, 2006, **235**, 95–104.

- 29 K. Abraham, S. Opfergelt, F. Fripiat, A.-J. Cavagna, J. T. M. De Jong, S. F. Foley, L. André and D. Cardinal, *Geostand. Geoanal. Res.*, 2008, **32**, 193–202.
- 30 R. M. G. Armytage, R. B. Georg, H. M. Williams and A. N. Halliday, *Geochim. Cosmochim. Acta*, 2012, **77**, 504–514, DOI: 10.1016/j.gca.2011.10.032.
- 31 M. A. Brzezinski and D. M. Nelson, *Deep Sea Res., Part I*, 1995, **42**, 1215–1237.
- 32 D. M. Karl and G. Tien, *Limnol. Oceanogr.*, 1992, **37**, 105–116.
- 33 A. Zhang, J. Zhang, R. Zhang and Y. Xue, *J. Anal. At. Spectrom.*, 2014, **12**, 2414–2418, DOI: 10.1039/C4JA00122B.
- 34 K. J. R. Rosman and P. D. P. Taylor, *Pure Appl. Chem.*, 1998, **70**, 217–236.
- 35 Y. Benjamini and Y. Hochberg, *Journal of the Royal Statistical Society*, 1995, **57**, 289–300.
- 36 K. J. F. Verhoeven, K. L. Simonsen and L. M. McIntyre, *Oikos*, 2005, **108**, 643–647.
- 37 H. J. Hughes, C. Delvigne, M. Korntheuer, J. de Jong, L. André and D. Cardinal, *J. Anal. At. Spectrom.*, 2011, **26**, 1892–1896.
- 38 M. H. Thiemens, *Science*, 1999, **283**, 341–345.
- 39 E. D. Young, A. Galy and H. Nagahara, *Geochim. Cosmochim. Acta*, 2002, **66**, 1095–1104.
- 40 D. M. Nelson, P. Tréguer, M. A. Brzezinski, A. Leynaert and B. Quéguiner, *Global Biogeochem. Cycles*, 1995, **9**, 359–372.
- 41 D. Cardinal, N. Savoye, T. W. Trull, F. Dehairs, E. E. Kopczynska, F. Fripiat, J.-L. Tison and L. André, *Mar. Chem.*, 2007, **106**, 46–62.
- 42 I. Closset, D. Cardinal, M. Rembauville, F. Thil and S. Blain, *Biogeosciences*, 2016, **13**, 6049–6066, DOI: 10.5194/bg-13-6049-2016.
- 43 J. Fietzke and M. Frische, *J. Anal. At. Spectrom.*, 2015, **31**, 234–244.